



## Removal of Cu<sup>2+</sup> from aqueous solution using three alkyl-amine-modified cellulose adsorbents prepared via Schiff base grafting

Yu Li<sup>a,b</sup>, Fei Wang<sup>a,b,\*</sup>

<sup>a</sup>International Innovation Center for Forest Chemicals, College of Chemical Engineering, Nanjing Forestry University, Jiangsu Key Lab for the Chemistry and Utilization of Agro-Forest Biomass, Nanjing 210037, China, Tel.: 13913869292/+86 (0) 25 85427649; email: hgwf@njfu.edu.cn (F. Wang), Tel.: 15754315614; email: 770216427@qq.com (Y. Li)

<sup>b</sup>Jiangsu Co-Innovation Center of Efficient Processing and Utilization of Forest Resources, College of Chemical Engineering, Nanjing Forestry University, Longpan Road 159, Nanjing 210037, China

Received 5 January 2022; Accepted 30 November 2022

### ABSTRACT

Alkyl-amine-modified cellulose adsorbents were synthesized by the oxidation reaction of cellulose with sodium periodate followed by a Schiff base reaction with taurine (DAC-SO<sub>3</sub>H), β-alanine (DAC-COOH), or β-cysteamine (DAC-SH). The adsorbents were characterized by elemental analysis, Fourier-transform infrared spectroscopy, and scanning electron microscopy; the results proved that cellulose had been modified successfully. The adsorption of Cu<sup>2+</sup> in the aqueous solutions by these three alkyl-amine-modified cellulose adsorbents was studied. The effects of the pH, Cu<sup>2+</sup> concentration, and adsorption time were also analyzed. The results confirmed that these three alkyl-amine-modified cellulose adsorbents had excellent adsorption efficiencies for the removal of Cu<sup>2+</sup> from wastewater.

*Keywords:* Alkyl-amine-modified cellulose adsorbent; Cu<sup>2+</sup>; Adsorption capacity

### 1. Introduction

Heavy metals persist in water and soil for a long time and do not degrade easily. During the ecological cycle, they accumulate in plants, animals, and even the human body leading to health issues. Timely and effective treatment of wastewater containing heavy metals is thus crucial. Material adsorption is an effective way to remove heavy metals. Versus other adsorbents, functionalized cellulose effectively adsorbs heavy metal ions through coordination and also remains very stable. Therefore, it is the most widely used heavy metal adsorbent in environmental science. However, due to the different functional groups on cellulose, the adsorption type and capacity for heavy metals vary. Therefore, with the development of functional cellulose adsorbents, it is necessary to explore their heavy metal adsorption properties [1,2]. In recent years, researchers

have tried to improve the adsorption efficiencies of biopolymers by grafting chelators to the polymers to enhance their chemical strength and metal chelation ability. Tran et al. [3] reported that carboxymethyl cellulose/sodium styrene sulfonate hydrogels can be used for the highly selective enrichment of Cr<sup>2+</sup> and Pb<sup>2+</sup>. The adsorption of Cu<sup>2+</sup> in wastewater was effectively achieved via carboxymethyl cellulose/thiosemicarbazide prepared by Ahmad et al. [4], which agreed with a pseudo-second-order kinetics model. The cellulose beads/glycine adsorbent prepared by Du et al. [5] exhibited good adsorption performances for Co<sup>2+</sup> and Cu<sup>2+</sup> under static adsorption conditions.

Copper is a common toxic heavy metal that often appears in industrial wastewater, such as from the machinery, metal, electrical, and light industries. With the discharge of wastewater, it can easily accumulate in various types of

\* Corresponding author.

biological tissue and can be absorbed by the human body through the digestive tract, thus leading to adverse effects to a variety of organs. If the copper content in the human body exceeds 1.5 mg/L, then it can easily cause liver cirrhosis and damage the nervous system [6–9]. Researchers have conducted extensive studies to solve the problem of high copper content in polluted water. The main method to remove  $\text{Cu}^{2+}$  is currently adsorption. Generally, adsorbent materials with large specific surface area or special functional groups are used to adsorb  $\text{Cu}^{2+}$  from aqueous solutions [10–12], for example, the carboxymethyl cellulose/thiosemicarbazide prepared by Ahmad et al. [4]. The maximum adsorption capacity of  $\text{Cu}^{2+}$  obtained using carboxymethyl cellulose/thiosemicarbazide was calculated based on the Langmuir model and was 144.92 mg/g.

Here, wood pulp cellulose was selected as a biopolymer. It tends to split into Schiff base intermediates at the C2 and C3 atoms. The insertion of taurine,  $\beta$ -alanine, or  $\beta$ -cysteamine in wood pulp cellulose increased the functionality, which in turn increased the metal chelation [4,13]. The preparation of alkyl-amine-modified cellulose-based nontoxic biosorbents (DAC- $\text{SO}_3\text{H}$ , DAC-COOH, and DAC-SH), and their adsorption performances for  $\text{Cu}^{2+}$  were studied. Various analyses were carried out: (i) The adsorption performances of the alkyl-amine-modified cellulose adsorbents for  $\text{Cu}^{2+}$  in wastewater were evaluated. (ii) Experimental conditions, such as the pH, concentration of  $\text{Cu}^{2+}$ , and contact time, were analyzed by different batch processing methods. (iii) Various models were examined for the adsorption equilibrium and kinetics, and their applicability was analyzed.

## 2. Materials and methods

### 2.1. Chemicals

All reagents and solvents were commercially available and used without further purification unless otherwise specified. The wood pulp used here was obtained from the Light Industry and Food Engineering College. Sodium periodate ( $\text{NaIO}_4$ , 99.5%) and ethylene glycol (99.5%) were purchased from Hushi (Shanghai, China). Taurine (99%),  $\beta$ -alanine (99%), and  $\beta$ -cysteamine (95%) were received from Aladdin (Shanghai, China). Methanol and ethanol were obtained from Nanhua (Nanjing, China). Ultrapure water was used in all the experiments.

### 2.2. Pretreatment of wood pulp

First, 20 g of dried wood pulp was added to 5 L of 12% NaOH. The mixture was then stirred intensely at room temperature for 24 h. The wood pulp was collected from the mixture by filtration. The treated wood pulp cellulose was washed with ultrapure water, after which it was freeze-dried and stored as the raw material [5].

### 2.3. Preparation of dialdehyde cellulose

Dialdehyde cellulose (DAC) was prepared by an improved oxidation process with  $\text{NaIO}_4$  [5,14–19]. Briefly, 4 g of wood pulp cellulose was dispersed in 200 mL of

ultrapure water, which was then mixed with 26.4 g of  $\text{NaIO}_4$  (about 5 mol per mol of anhydrous glucose units). The reaction mixture containing  $\text{NaIO}_4$  was wrapped in aluminum foil to avoid exposure of the reaction mixture to light. The reaction mixture was stirred violently for 10 d in the dark at room temperature. DAC was produced due to oxidation. Finally, the reaction was quenched by adding ethylene glycol to the reaction system, and the resulting DAC product was washed repeatedly with ultrapure water to provide DAC.

### 2.4. Determination of aldehyde content

According to a previously reported procedure [14–16], DAC samples were converted into aldoxime by a Schiff base reaction with hydroxylamine, and the elemental compositions (C, H, and N) were analyzed. First, 100 mg of DAC, 40 mL of acetate buffer (pH 4.5), and 1.65 mL of hydroxylamine solution (aqueous, 50 wt.%) were added to a 100-mL round-bottomed flask. The reaction mixture was stirred at room temperature for 24 h. The product was thoroughly washed with water and freeze-dried prior to elemental analysis. The degree of oxidation (DO) represents the percentage of 2,3-alcohols in the anhydroglucose units that have been transformed into their corresponding aldehydes. The highest degree of oxidation (i.e., 100%) corresponds to all anhydroglucose units being converted to the corresponding noncyclic 2,3-dialdehyde structure. This corresponds to approximately 12.5 mmol of aldehyde groups per gram of cellulose.

### 2.5. Preparation of Schiff-base amino-modified porous cellulose

The amino-modified porous cellulose was prepared by a Schiff-base reaction. The chemical route is described as follows [5,20]. First, 12 mmol of taurine,  $\beta$ -alanine, and  $\beta$ -cysteamine was dissolved into 45 mL of methyl alcohol solvent. The mixture was then poured into a 100-mL 2-neck flask, followed by 320 mg of porous cellulose. The reaction system was heated at 60°C and kept for 12 h under continuous stirring, which led to the generation of amino-modified cellulose. Finally, the modified porous cellulose was washed with pure water and dried in vacuum at -45°C.

### 2.6. Characterization

The elemental composition of grafted cellulose was analyzed by an elemental analyzer (EA), and the degree of substitution was determined. The chemical bonds of the samples were analyzed by Fourier-transform infrared spectroscopy (FTIR), and the microscopic morphologies of the porous cellulose were investigated by scanning electron microscopy (SEM).

### 2.7. Adsorption experiments

The adsorption of  $\text{Cu}^{2+}$  on the amino-modified porous cellulose was measured by batch experiments at different pH values (2.0–6.0). The adsorption equilibrium isotherms were obtained over a concentration range of 10–1,000 mg/L. The adsorption kinetics at different time

intervals of 0–3 h were analyzed. The experiments were carried out in screw-thread bottles containing 10 mg of amino-modified porous cellulose and 10 mL of metal ion solution oscillated at room temperature for a specified time. The initial pH values were adjusted with 1 M HNO<sub>3</sub> and 1 M NaOH solutions. The cellulose was separated from the solution by filtration after the adsorption experiments. Meanwhile, the residual heavy metal concentrations in solution were determined by inductively coupled plasma mass spectrometry (ICP-MS). The adsorption capacity of cellulose toward heavy metal ions was calculated according to the following equation:

$$q = \frac{(C_2 - C_1)V}{M} \quad (1)$$

where  $q$  is equilibrium adsorption capacity of the metal ions (mg/g),  $C_1$  and  $C_2$  (mg/L) are the equilibrium and initial metal ion concentrations in solution, respectively,  $V$  (L) is the volume of the adsorbed solution, and  $M$  (g) is the weight of dried modified cellulose.

### 3. Results and discussion

Unfunctionalized DAC was prepared by periodate oxidation of cellulose from wood pulp in water, as previously described [15]. The formed porous DAC was highly oxidized (the degree of oxidation was about 99%, corresponding to 12.1 mmol aldehyde/g cellulose), which is very close to the theoretical value (100% oxidation corresponds to 12.5 mmol aldehyde /g cellulose). These results suggest that the oxidation process was successful and conducive to the next step of the reaction. Elemental analysis data are shown in Table 1.

#### 3.1. Characterization

Elemental analyses of the three modified cellulose samples were carried out, and the results are shown in Table 2. The contents of C, H, N, and S were measured by an elemental analyzer, and the contents of O were obtained by calculation. According to the calculation, the degree of substitution (DS) of DAC-SO<sub>3</sub>H, DAC-COOH, and DAC-SH was 0.53, 0.62, and 0.52, respectively. In conclusion, under the same experimental conditions, taurine, β-alanine and β-cysteamine react differently with DAC, which may be related to the types of functional groups.

The synthesis route of the amino-modified cellulose is shown in Fig. 1. Taurine, β-alanine, and β-cysteamine were

grafted onto the surface of the cellulose through a two-step method. First, sodium periodate broke the C–C covalent bonds at the C2 and C3 positions on the cellulose and oxidized it to dialdehyde cellulose. Schiff base reactions were conducted with taurine, β-alanine, and β-cysteamine in the organic environment to obtain adsorbents DAC-SO<sub>3</sub>H, DAC-COOH, and DAC-SH, respectively. Their metal ion adsorption characteristics were examined next. Only the functional groups of the three reactants are different, and the reaction process is simple. Non-experimental factors have little influence on the product formation, which is more conducive to comparing the adsorption performance of the three functional groups to heavy metal ions.

The SEM images of the cellulose before and after modification are shown in Fig. 2. Fig. 2A shows that the cellulose fiber with eucalyptus pulp board as the raw material was composed of dry, straight, and rod-like wrinkled surfaces. Inspection by eye shows that the original material is layered, compact, and difficult to disperse. The cellulose surface changed significantly after the reaction of dialdehyde cellulose with taurine, that is, as if it had been corroded (Fig. 2B). For the β-alanine reaction, a relatively uniform and dense helical spatial structure formed on the surface of the cellulose chain (Fig. 2C). In addition, the hardness of the oxidized cellulose fibers decreased gradually with reaction of β-cysteamine, and the structure of the cellulose was destroyed, which significantly reduced the fiber sizes (Fig. 2D). The three graft products have clear microscopic differences. On the macro level, DAC-SO<sub>3</sub>H and DAC-COOH are slightly similar and show a loose three-dimensional structure. DAC-SH has an uneven size and irregularly shaped block structure. The similarity is that they are easily dispersed in water during the adsorption experiment. This may be because all three functional groups are hydrophilic.

To better understand the modifications, the raw material (cell), oxidation product dialdehyde cellulose (DAC), and grafted products (DAC-SO<sub>3</sub>H, DAC-COOH, and DAC-SH) were examined by FTIR analysis (Fig. 3). The FTIR spectrum of the DAC showed that a characteristic peak appeared at 1,735 cm<sup>-1</sup> and was ascribed to the oxidation reaction that converted –OH groups (3,375 cm<sup>-1</sup>) at C2 and C3 positions into –CHO groups [5,16]. In addition, a new peak of DAC appeared at 885 cm<sup>-1</sup> and was attributed to the further reaction between the –CHO and –OH terminals [5,14]. The main characteristic bands of DAC-SO<sub>3</sub>H are also shown at 1,030 and 994 cm<sup>-1</sup> (SO<sub>3</sub>H groups) and at 1,195 and 1,113 cm<sup>-1</sup> (S=O stretching) [3].

Table 1  
EA results and DO of cellulose before and after oxidation

Sample	Results					DO [CHO]	
	%C	%H	%N	%S	%O	(mmol/g)	
Cellulose	42.99	6.416	1.03	0.085	49.48		
Aldoxime	33.14	5.201	12.74	0.06	48.86	0.99	12.1

DO, degree of oxidation; EA, elemental analysis.

Table 2  
EA results and DS of cellulose before and after modification

Sample	Results					DS
	%C	%H	%N	%S	%O	
Cellulose	42.99	6.416	1.03	0.085	49.48	
DAC-SO <sub>3</sub> H	34.14	2.902	5.18	12.31	45.47	0.53
DAC-COOH	44.23	4.042	6.59	0.164	44.97	0.62
DAC-SH	43.53	6.614	8.48	19.86	21.52	0.52

DS, degree of substitution; EA, elemental analysis.

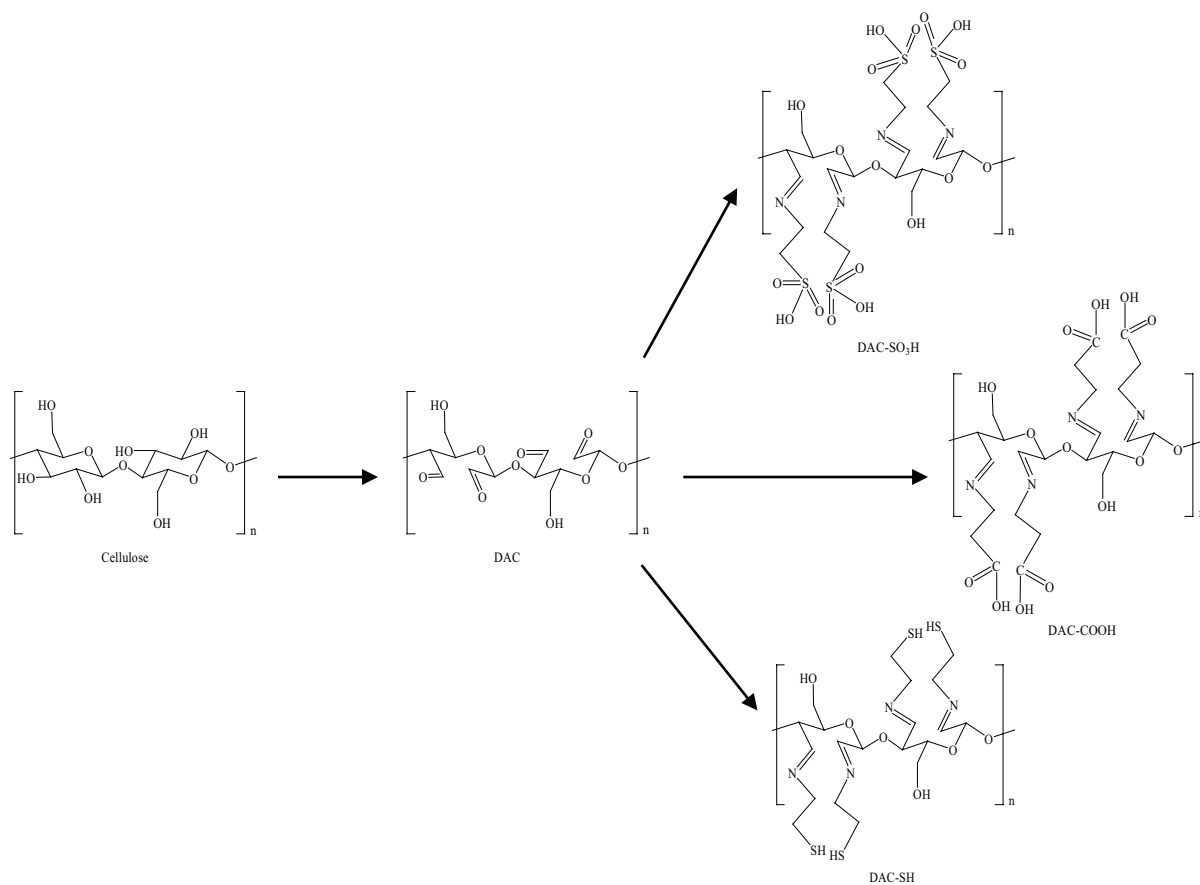


Fig. 1. Preparation roadmap of DAC-SO<sub>3</sub>H, DAC-COOH, and DAC-SH.

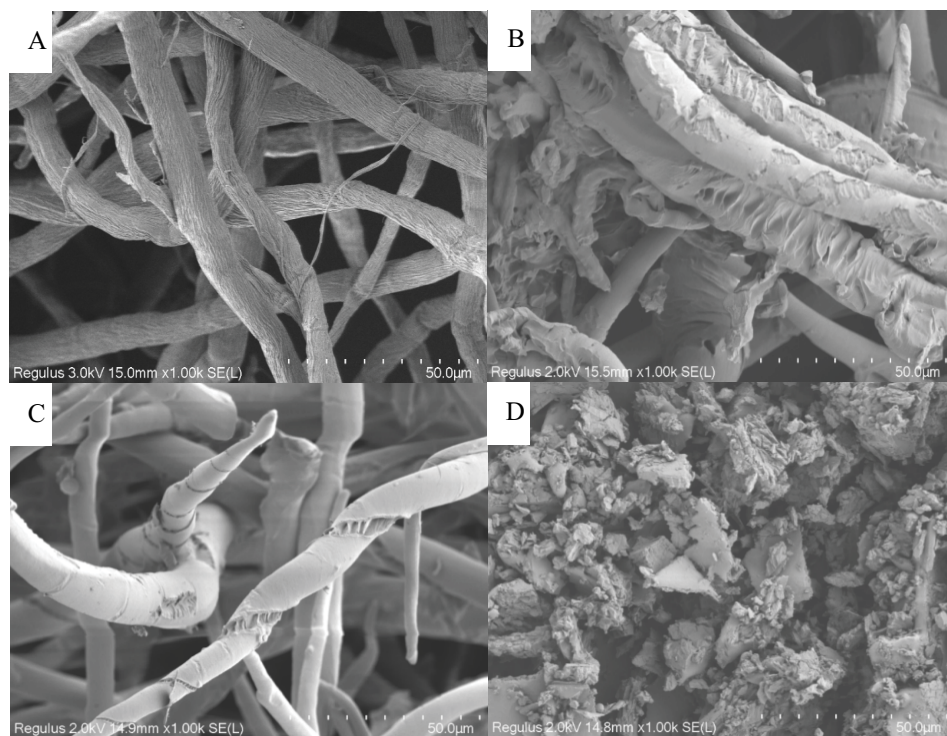


Fig. 2. Scanning electron microscopy (SEM) images of cellulose at different stages: raw material (A), DAC-SO<sub>3</sub>H (B), DAC-COOH (C), and DAC-SH (D).

A new absorption band appeared at  $2,642\text{ cm}^{-1}$  after the formation of the DAC-SH, which was due to the stretching vibrations of the  $-\text{SH}$  band [21]. In the FTIR spectrum of the DAC-COOH, several new absorption bands appeared at  $2,630$ ;  $1,250$  and  $1,150\text{ cm}^{-1}$  and correspond to the combined peaks of C–O and O–H (in plane), the stretching vibration peak of C–O, and the peak of carbonyl carbon  $=\text{C}-\text{C}$  [22,23]. The comparative analysis in Fig. 3 shows that the characteristic peaks of the aldehyde group are clear after the original material is oxidized into dialdehyde cellulose. The products obtained by the subsequent Schiff base reaction have their own characteristic peaks, which proves that the experiment was successful.

SEM and FTIR was used to propose a mechanism of one-step growth of porous cellulose via the oxidation reaction of  $\text{NaO}_4$  in aqueous phase. First, sodium peroxide-mediated oxidation of the cellulose fibers was a highly selective reaction, which oxidized the OH terminals of the C2 and C3 positions on the cellulose fibers to form the corresponding aldehydes [24]. Further oxidation promoted the swelling of cellulose oxide fibers in solution. This was due to the subsequent reactions: During oxidation, the crystalline cellulose was transformed into long and amorphous oxidized cellulose chains and formed the end of the dialdehyde; this surprising finding contrasted with Kim's previous report, in which oxidation often broke cellulose fibers into short fragments [24]. During the process of curing, the oxidized cellulose long chains were reassembled by hydrogen bonding interactions, thus forming a three-dimensional spatial structure. Elemental analysis showed that the content of the aldehyde groups on the oxidized cellulose sample was about  $12.1\text{ mmol/g}$ , which provided sufficient active sites for the immobilization of adsorption ligands.

### 3.2. Adsorption evaluation of three alkyl-amine-modified cellulose samples

An adsorbent is generally composed of a carrier and adsorption ligand groups. The adsorption of special

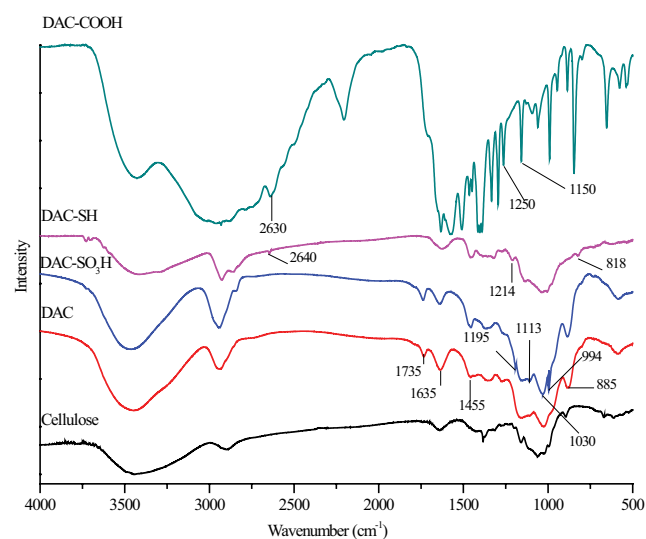


Fig. 3. Fourier-transform infrared spectroscopy (FTIR) spectra.

substances is determined by the fixed ligand groups on the carrier. In this context, taurine,  $\beta$ -alanine, and  $\beta$ -cysteamine were selected as adsorption ligands because of their simple and non-toxic chemical structures and the presence of N, S, and O atoms with lone electron pairs [24]. On the basis of the Schiff base reaction, taurine,  $\beta$ -alanine, and  $\beta$ -cysteamine were modified onto porous cellulose to prepare several new cationic adsorbents. The adsorption performances of the amino-modified adsorbents for heavy metal ions in wastewater were evaluated.

### 3.3. Adsorption effect of pH

The pH value of the solution affected not only the protonation degree of the adsorbed ligands but also the formation of heavy metal ions in solution. Thus, it played an important role in the adsorption behaviors of the adsorbents. We carried out a series of batch equilibrium experiments using a  $\text{Cu}^{2+}$  solution with an initial concentration of  $10\text{ mg/L}$  to determine the effect of the pH on the adsorption of heavy metal ions by these adsorbents. The  $\text{Cu}^{2+}$  hydrolyzed when the pH of the solution was greater than 6 leading to precipitation. Therefore, a dilute  $\text{HNO}_3$  or  $\text{NaOH}$  solution was used to adjust the pH to 2.0–6.0 (Fig. 4).

Fig. 4 shows that the adsorption capacities of three kinds of alkyl-amine-modified cellulose for  $\text{Cu}^{2+}$  first increased and then decreased with increasing pH. When the pH value increased from 2.0 to 4.5, the adsorption capacity increased gradually. The adsorption capacity decreased slightly when the pH increased to 6.0. However, the adsorption capacity was generally higher when the pH was 4.5 to 5.5, and thus a pH range of 4.5–5.5 was selected for further adsorption experiments.

### 3.4. Adsorption isotherms

Adsorption isotherm analysis is of great significance for determining the adsorption capacity and determining the adsorption properties of the adsorbents. Langmuir and Freundlich isotherm models were used to explain the equilibrium adsorption data. The Langmuir isotherm was based on the assumption that a monolayer adsorbs on a

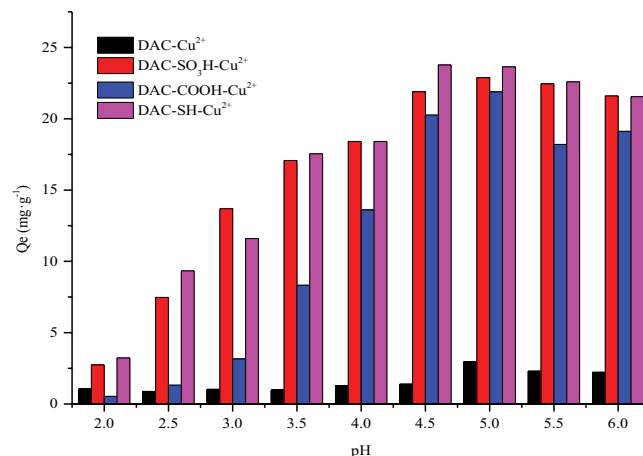


Fig. 4. Effect of initial pH on adsorption capacities of adsorbents.

surface containing a limited number of adsorption sites, and the adsorbate does not migrate on the surface plane. The Langmuir isotherm model is as follows:

$$\text{Langmuir: } \frac{C_e}{Q_e} = \frac{C_e}{Q_m} + \frac{1}{Q_m K_L} \quad (2)$$

where  $C_e$  is the equilibrium concentration (mg/L),  $Q_e$  is the amount of equilibrium adsorbate (mg/g),  $K_L$  is the “affinity” parameter (L/mg), and  $Q_m$  is the “capacity” parameter (mg/g).

The Freundlich isotherm model assumes the surface energy on the surface of the adsorbent is heterogeneous. The Freundlich isotherm model is as follows:

$$\text{Freundlich: } Q_e = K_F C_e^{1/n} \quad (3)$$

where  $K_F$  and  $n$  are Freundlich parameters.

Fig. 5 shows the adsorption isotherms curves of  $\text{Cu}^{2+}$  by the DAC, DAC- $\text{SO}_3\text{H}$ , DAC-COOH, and DAC-SH adsorbents. The adsorption capacities of the three amino-modified cellulose samples for  $\text{Cu}^{2+}$  increased with

increasing  $\text{Cu}^{2+}$  concentration until saturation. The saturated adsorption capacities ( $Q_m$ ) of the DAC, DAC- $\text{SO}_3\text{H}$ , DAC-COOH, and DAC-SH for  $\text{Cu}^{2+}$  were 17.83, 178.59, 140.85, and 119.30 mg/g, respectively. The Langmuir and Freundlich models [Eqs. (2) and (3), respectively] were used to fit the experimental data to further understand the adsorption behaviors of three amino-modified cellulose samples for  $\text{Cu}^{2+}$ . The fitting results are shown in Table 3.

The Langmuir isotherm adsorption constant  $K_L$  values were  $0 < K_L < 1$ , which indicated that  $\text{Cu}^{2+}$  was easily adsorbed onto the surfaces of the three amino-modified cellulose samples. According to the Langmuir formula, the maximum adsorption capacities ( $Q_m$ ) of the DAC- $\text{SO}_3\text{H}$ , DAC-COOH, and DAC-SH for  $\text{Cu}^{2+}$  were 212.77, 166.11, and 136.43 mg/g, respectively, which are 10.13, 7.91, and 6.50-fold higher than that of the DAC (21 mg/g). The results indicated that under the same reaction conditions, the adsorption capacities of the amino-modified cellulose samples for  $\text{Cu}^{2+}$  were significantly improved vs. DAC. The values were on the order of DAC- $\text{SO}_3\text{H}$  > DAC-COOH > DAC-SH. According to the fitting degree  $R^2$ , the fitting effect of the Langmuir model was better than that of the Freundlich model, thus indicating that the adsorption process of

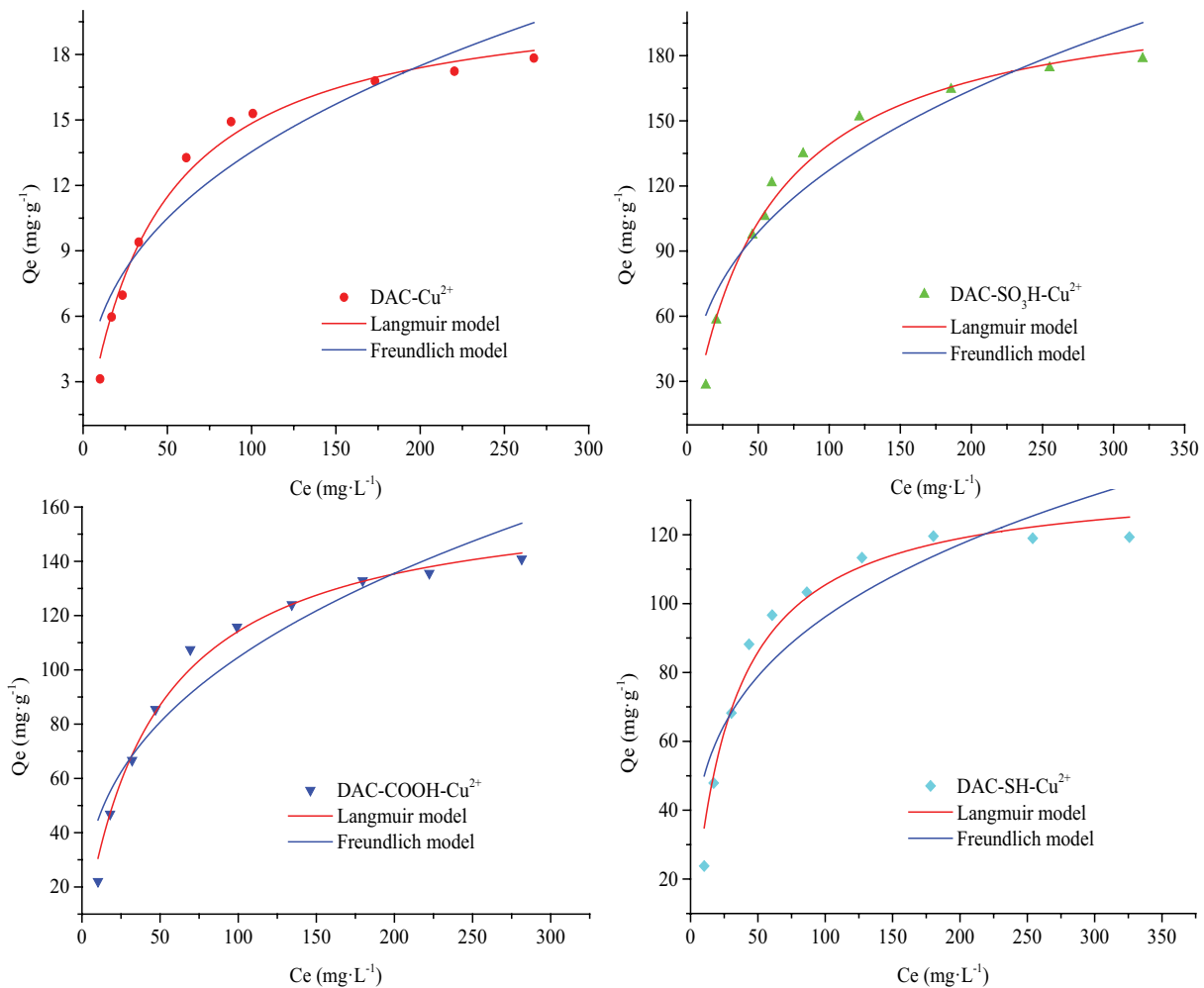


Fig. 5. Adsorption isotherms of  $\text{Cu}^{2+}$ .

Table 3  
Fitted results of Langmuir and Freundlich models

	Langmuir			Freundlich		
	$K_L$ (mg/L)	$Q_m$ (mg/g)	$R^2$	$K_F$ (mg <sup>1-1/n</sup> L <sup>1/n</sup> .g <sup>-1</sup> )	$n$	$R^2$
DAC	0.0241	21.00	0.9874	2.4818	2.714	0.8942
DAC-SO <sub>3</sub> H	0.0189	212.77	0.9823	23.4973	2.725	0.8840
DAC-COOH	0.0220	166.11	0.9893	18.7132	2.676	0.9042
DAC-SH	0.0340	136.43	0.9709	25.8158	3.503	0.8123

Table 4  
Fitted results of pseudo-first-order and pseudo-second-order kinetics models

	Pseudo-first-order			Pseudo-second-order		
	$k_1$ (min <sup>-1</sup> )	$q_e$ (mg/g)	$R^2$	$k_2$ (g/mg·min)	$q_e$ (mg/g)	$R^2$
DAC	0.1727	12.58	0.9632	0.0078	13.81	0.9746
DAC-SO <sub>3</sub> H	0.0303	100.97	0.9258	0.0015	111.80	0.9841
DAC-COOH	0.2059	83.09	0.9400	0.0013	92.68	0.9908
DAC-SH	0.2802	88.08	0.9406	0.0018	96.76	0.9819

Cu<sup>2+</sup> on the three kinds of amino-modified cellulose was mainly dominated by monomolecular chemisorption.

### 3.5. Adsorption kinetics

The effect of the metal ion concentration on the adsorption rate is important to understand the adsorption mechanism. Two kinetics models were used to fit the adsorption kinetics data to quantify the change of the adsorption capacity over time and evaluate the kinetics parameters for different metal ion concentrations: a pseudo-first-order kinetic model:

$$\log(q_e - q_t) = \log q_e - \frac{k_1 t}{2.303} \quad (4)$$

Pseudo-second-order kinetic model:

$$\frac{t}{q_t} = \frac{1}{k_2 q_e^2} + \frac{t}{q_e} \quad (5)$$

where  $q_t$  is the adsorption capacity at time  $t$  (mg/g), and  $k_1$  and  $k_2$  are the adsorption rate constants of the pseudo-first-order (min<sup>-1</sup>) and pseudo-second-order (g/mg·min) reactions, respectively. The results are shown in Fig. 6 and Table 4.

Fig. 6 shows the adsorption kinetics curve of the Cu<sup>2+</sup> on the three kinds of amino-modified cellulose. The adsorption amount of Cu<sup>2+</sup> by the three amino-modified cellulose samples increased and finally reached adsorption equilibrium with increasing time. The experimental adsorption data showed that the adsorption was very fast and reached a maximum adsorption capacity within 60 min. It reached an adsorption equilibrium after about 100 min.

The pseudo-first-order and pseudo-second-order dynamics models were used to fit the experimental data,

and the fitting results are shown in Table 4. According to the pseudo-first-order kinetics constants, the Cu<sup>2+</sup> adsorption rates for the DAC-SO<sub>3</sub>H, DAC-COOH, and DAC-SH were 0.0303, 0.2059, and 0.2802 min<sup>-1</sup>, respectively. The pseudo-second-order kinetics constants show that the adsorption rates of Cu<sup>2+</sup> for the DAC-SO<sub>3</sub>H, DAC-COOH, and DAC-SH were 0.0015, 0.0013, and 0.0018 g/mg·min, respectively. The fitting result ( $R^2$ ) of the pseudo-second-order kinetics model was better, and the experimental data point  $q_e$  was close to the theoretical value of the fitted line  $q_e$ . These results indicated that the pseudo-second-order kinetics model could better describe the adsorption process of Cu<sup>2+</sup> for the three kinds of amino-modified cellulose. The results showed that the adsorption of the three amino-modified cellulose types was controlled by chemisorption, which was determined by the concentration of Cu<sup>2+</sup> and the number of active adsorption sites on the modified cellulose.

## 4. Conclusions

The Sulfonic acid group, carboxyl group, and sulfhydryl group are popular coordination groups of heavy metal ions. The original intent of this paper was to compare the adsorption performance of these three different functional groups on heavy metal ions. Therefore, three reactants with the same main chain but different functional groups (taurine,  $\beta$ -alanine, and  $\beta$ -cysteamine) were selected as the grafting objects for the Schiff base reaction. Three kinds of amino-modified cellulose (DAC-SO<sub>3</sub>H, DAC-COOH, and DAC-SH) were similarly prepared. Only the functional groups of reactants are different—the reaction steps are simple and robust. Our conclusions are statistically sound and consistent with the premise of this study. We further confirmed the practical feasibility of the approach using computational chemistry [25].

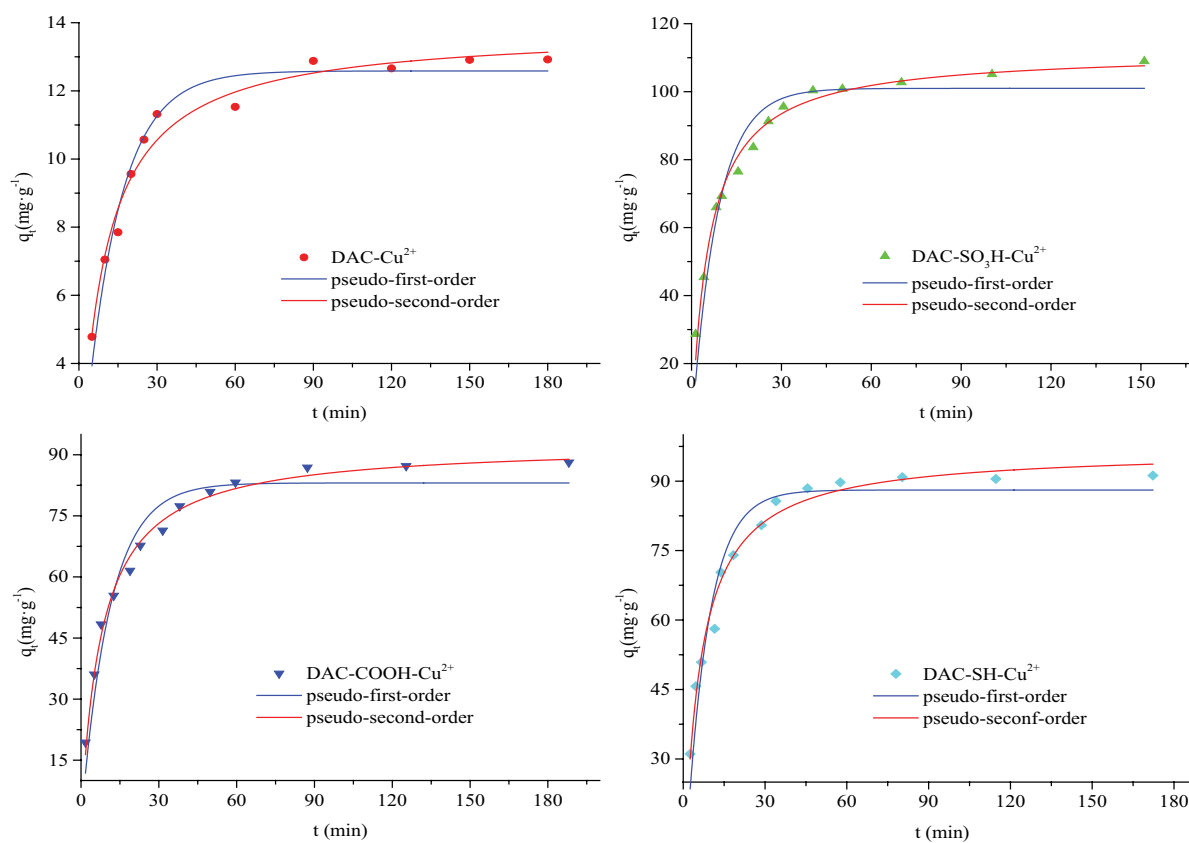


Fig. 6. Adsorption kinetics of  $\text{Cu}^{2+}$ .

EA, SEM, and FTIR characterization showed that taurine ( $-\text{SO}_3\text{H}$ ),  $\beta$ -alanine ( $-\text{COOH}$ ), and  $\beta$ -cysteamine ( $-\text{SH}$ ) were successfully bonded to the cellulose. The adsorbents DAC- $\text{SO}_3\text{H}$ , DAC-COOH, and DAC-SH were then used for heavy metal ion adsorption experiments to explore the adsorption properties of the three functional groups. Several parameters were investigated, including pH, adsorption isotherm, and kinetics. The optimal pH range of adsorption was 4.5–5.5. In addition, the  $\text{Cu}^{2+}$  adsorption isotherm and kinetics data of the DAC- $\text{SO}_3\text{H}$ , DAC-COOH, and DAC-SH were consistent with the Langmuir model and pseudo-second-order model, respectively. The  $\text{Cu}^{2+}$  adsorption capacities of the three amine-modified cellulose adsorbents were DAC- $\text{SO}_3\text{H}$  > DAC-COOH > DAC-SH. These results confirmed that the modified cellulose could be used as an ideal adsorbent for heavy metal removal from wastewater. This work provided a reference for the removal of heavy metal ions in water by adsorption, especially under the increasing demand from regulatory authorities to move to more environmentally friendly chemistry. In weakly acidic conditions, DAC- $\text{SO}_3\text{H}$  showed stronger adsorption capacity for  $\text{Cu}^{2+}$ , that is, up to 212.77 mg/g. This material can be applied to sewage treatment and industrial waste recycling.

### Symbols

$C_1, C_2$  — Equilibrium and initial metal ion concentrations in solution, mg/L

$C_e$	—	Equilibrium concentration, mg/L
$k_1, k_2$	—	Adsorption rate constants of the pseudo-first-order ( $\text{min}^{-1}$ ) and pseudo-second-order ( $\text{g}/\text{mg}\cdot\text{min}$ ) reactions
$K_f, n$	—	Freundlich parameters
$K_L$	—	"Affinity" parameter, L/mg
$M$	—	Weight of dried modified cellulose, g
$q$	—	Equilibrium adsorption capacity of the metal ions, mg/g
$Q_e$	—	Amount of equilibrium adsorbate, mg/L
$Q_m$	—	"Capacity" parameter, mg/g
$q_t$	—	Adsorption capacity at time $t$ , mg/g
$R^2$	—	Fitting degree
$V$	—	Volume of the adsorbed solution, L

### References

- [1] Y. Peng, H. Huang, Y. Zhang, C. Kang, S. Chen, L. Song, D. Liu, C. Zhong, A versatile MOF-based trap for heavy metal ion capture and dispersion, *Nat. Commun.*, 9 (2018) 187, doi: 10.1038/s41467-017-02600-2.
- [2] I.M. El-Nahhal, N.M. El-Ashgar, A review on polysiloxane-immobilized ligand systems: synthesis, characterization and applications, *J. Organomet. Chem.*, 692 (2007) 2861–2886.
- [3] T.H. Tran, H. Okabe, Y. Hidaka, K. Hara, Removal of metal ions from aqueous solutions using carboxymethyl cellulose/sodium styrene sulfonate gels prepared by radiation grafting, *Carbohydr. Polym.*, 157 (2017) 335–343.
- [4] M. Ahmad, K. Manzoor, S. Ahmad, S. Ikram, Preparation, kinetics, thermodynamics, and mechanism evaluation of thiosemicarbazide modified green carboxymethyl cellulose

- as an efficient Cu(II) adsorbent, *J. Chem. Eng. Data*, 63 (2018) 1905–1916.
- [5] K. Du, S. Li, L. Zhao, L. Qiao, H. Ai, X. Liu, One-step growth of porous cellulose beads directly on bamboo fibers via oxidation-derived method in aqueous phase and their potential for heavy metal ions adsorption, *ACS Sustainable Chem. Eng.*, 6 (2018) 17068–17075.
- [6] H. Gaete Olivares, N. Moyano Lagos, C. Jara Gutierrez, R. Carrasco Kittelsen, G. Lobos Valenzuela, M.E. Hidalgo Lillo, Assessment oxidative stress biomarkers and metal bioaccumulation in macroalgae from coastal areas with mining activities in Chile, *Environ. Monit. Assess.*, 188 (2016) 25, doi: 10.1007/s10661-015-5021-5.
- [7] S.E. Sabatini, Á.B. Juárez, M.R. Eppis, L. Bianchi, C.M. Luquet, M. del Carmen Ríos de Molina, Oxidative stress and antioxidant defenses in two green microalgae exposed to copper, *Ecotoxicol. Environ. Saf.*, 72 (2009) 1200–1206.
- [8] M.D. Machado, E.V. Soares, Short- and long-term exposure to heavy metals induced oxidative stress response in *Pseudokirchneriella subcapitata*, *Clean Soil Air Water*, 44 (2016) 1578–1583.
- [9] R. Pandey, G. Zinta, H. AbdElgawad, A. Ahmad, V. Jain, I.A. Janssens, Physiological and molecular alterations in plants exposed to high [CO<sub>2</sub>] under phosphorus stress, *Biotechnol. Adv.*, 33 (2015) 303–316.
- [10] G.A. Adebisi, Z.Z. Chowdhury, P.A. Alaba, Equilibrium, kinetic, and thermodynamic studies of lead ion and zinc ion adsorption from aqueous solution onto activated carbon prepared from palm oil mill effluent, *J. Cleaner Prod.*, 148 (2017) 958–968.
- [11] Z. Li, Z. Wang, C. Wang, S. Ding, F. Li, H. Lin, Preparation of magnetic resin microspheres M-P(MMA-DVB-GMA) and the adsorption property to heavy metal ions, *Appl. Surf. Sci.*, 496 (2019) 143708, doi: 10.1016/j.apsusc.2019.143708.
- [12] B. Zhao, H. Jiang, Z. Lin, S. Xu, J. Xie, A. Zhang, Preparation of acrylamide/acrylic acid cellulose hydrogels for the adsorption of heavy metal ions, *Carbohydr. Polym.*, 224 (2019) 115022, doi: 10.1016/j.carbpol.2019.115022.
- [13] M. Ahmad, S. Ahmed, B.L. Swami, S. Ikram, Preparation and characterization of antibacterial thiosemicarbazide chitosan as efficient Cu(II) adsorbent, *Carbohydr. Polym.*, 132 (2015) 164–172.
- [14] J. Lindh, D.O. Carlsson, M. Strømme, A. Mihrianyan, Convenient one-pot formation of 2,3-dialdehyde cellulose beads via periodate oxidation of cellulose in water, *Biomacromolecules*, 15 (2014) 1928–1932.
- [15] J. Lindh, C. Ruan, M. Strømme, A. Mihrianyan, Preparation of porous cellulose beads via introduction of diamine spacers, *Langmuir*, 32 (2016) 5600–5607.
- [16] U.-J. Kim, S. Kuga, M. Wada, T. Okano, T. Kondo, Periodate oxidation of crystalline cellulose, *Biomacromolecules*, 1 (2000) 488–492.
- [17] E.B. Strong, C.W. Kirschbaum, A.W. Martinez, N.W. Martinez, Paper miniaturization via periodate oxidation of cellulose, *Cellulose*, 25 (2018) 3211–3217.
- [18] F.F. Lu, H.Y. Yu, Y. Zhou, J.M. Yao, Spherical and rod-like dialdehyde cellulose nanocrystals by sodium periodate oxidation: optimization with double response surface model and templates for silver nanoparticles, *EXPRESS Polym. Lett.*, 10 (2016) 965–976.
- [19] L. Zhu, Y. Liu, Z. Jiang, E. Sakai, J. Qiu, P. Zhu, Highly temperature resistant cellulose nanofiber/polyvinyl alcohol hydrogel using aldehyde cellulose nanofiber as cross-linker, *Cellulose*, 26 (2019) 5291–5303.
- [20] R.S. Jagadish, K.N. Divyashree, P. Viswanath, P. Srinivas, B. Raj, Preparation of N-vanillyl chitosan and 4-hydroxybenzyl chitosan and their physico-mechanical, optical, barrier, and antimicrobial properties, *Carbohydr. Polym.*, 87 (2012) 110–116.
- [21] Z. Yang, H. Liu, J. Li, K. Yang, Z. Zhang, F. Chen, B. Wang, High-throughput metal trap: sulfhydryl-functionalized wood membrane stacks for rapid and highly efficient heavy metal ion removal, *ACS Appl. Mater. Interfaces*, 12 (2020) 15002–15011.
- [22] S. Kumari, G.S. Chauhan, New cellulose–lysine Schiff-base-based sensor–adsorbent for mercury ions, *ACS Appl. Mater. Interfaces*, 6 (2014) 5908–5917.
- [23] A. Daochalermwong, N. Chanka, K. Songsrirote, P. Dittanet, C. Niamnuay, A. Seubsai, Removal of heavy metal ions using modified celluloses prepared from pineapple leaf fiber, *ACS Omega*, 5 (2020) 5285–5296.
- [24] E. Schacht, B. Bogdanov, A.V.D. Bulcke, N. De Rooze, Hydrogels prepared by crosslinking of gelatin with dextran dialdehyde, *React. Funct. Polym.*, 33 (1997) 109–116.
- [25] I.H.S. Ribeiro, D.T. Reis, D.H. Pereira, A DFT-based analysis of adsorption of Cd<sup>2+</sup>, Cr<sup>3+</sup>, Cu<sup>2+</sup>, Hg<sup>2+</sup>, Pb<sup>2+</sup>, and Zn<sup>2+</sup>, on vanillin monomer: a study of the removal of metal ions from effluents, *J. Mol. Model.*, 25 (2019) 267, doi: 10.1007/s00894-019-4151-z.